Precipitation over eastern South America and the South Atlantic Sea surface temperature during neutral ENSO periods

Rodrigo J. Bombardi, Leila M. V. Carvalho, Charles Jones & Michelle S. Reboita

Climate Dynamics
Observational, Theoretical and Computational Research on the Climate System

ISSN 0930-7575
Volume 42
Combined 5-6

Clim Dyn (2014) 42:1553-1568
DOI 10.1007/s00382-013-1832-7

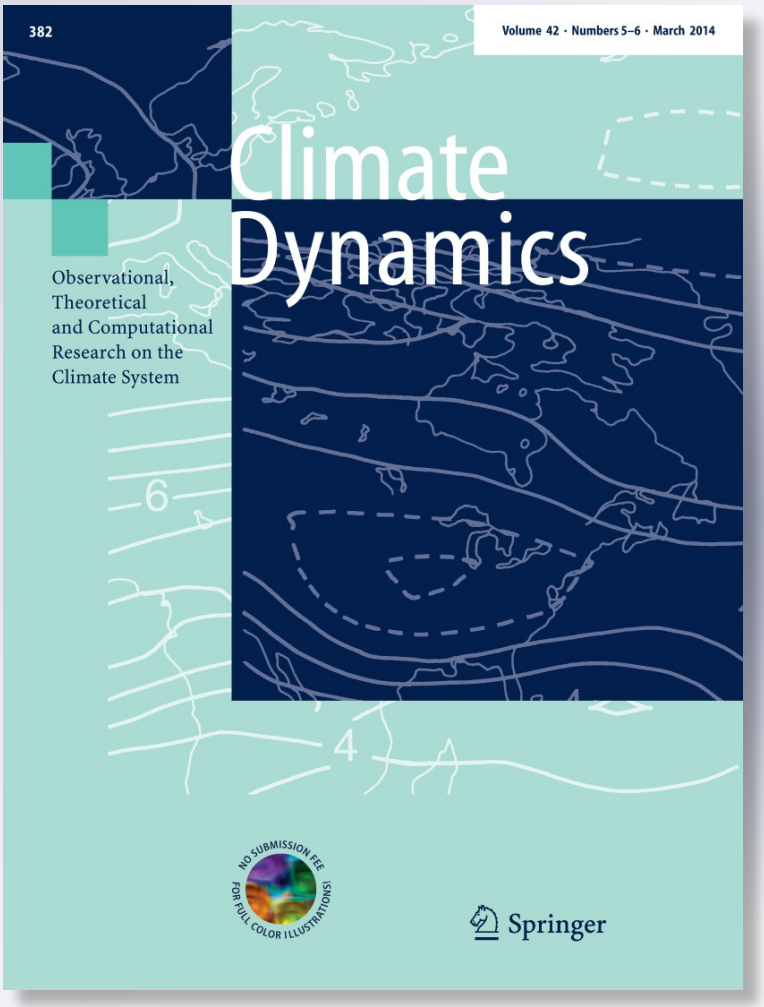

Springer

Clim Dyn (2014) 42:1553–1568
DOI 10.1007/s00382-013-1832-7

Precipitation over eastern South America and the South Atlantic Sea surface temperature during neutral ENSO periods

Rodrigo J. Bombardi · Leila M. V. Carvalho · Charles Jones · Michelle S. Reboita

Received: 6 November 2012 / Accepted: 4 June 2013 / Published online: 15 June 2013

Abstract The dominant mode of coupled variability over the South Atlantic Ocean is known as "South Atlantic Dipole" (SAD) and is characterized by a dipole in sea surface temperature (SST) anomalies with centers over the tropical and the extratropical South Atlantic. Previous studies have shown that variations in SST related to SAD modulate large-scale patterns of precipitation over the Atlantic Ocean. Here we show that variations in the South Atlantic SST are associated with changes in daily precipitation over eastern South America. Rain gauge precipitation, satellite derived sea surface temperature and reanalysis data are used to investigate the variability of the subtropical and tropical South Atlantic and impacts on precipitation. SAD phases are assessed by performing Singular value decomposition analysis of sea level pressure and SST anomalies. We show that during neutral El Niño Southern Oscillation events, SAD plays an important role in modulating cyclogenesis and the characteristics of the South Atlantic Convergence Zone. Positive SST anomalies over the extratropical South Atlantic (SAD negative phase) are related to increased cyclogenesis near southeast Brazil as well as the migration of extratropical cyclones further north. As a consequence, these systems organize convection and increase precipitation over eastern South America.

Keywords SST · Precipitation · South Atlantic Dipole · South America · ENSO · Cyclones

R. J. Bombardi (✉) · L. M. V. Carvalho
Department of Geography, University of California, Santa Barbara, CA 93106-3060, USA
e-mail: bombardi@geog.ucsb.edu; bombardi@umail.ucsb.edu

L. M. V. Carvalho · C. Jones
Earth Research Institute, University of California, Santa Barbara, CA, USA

M. S. Reboita
Natural Resources Institute, Federal University of Itajubá, Itajubá, Brazil

1 Introduction

Eastern South America is under the influence of the South American Monsoon System (Zhou and Lau 1998). The onset of the rainy season in this region occurs between September and November (e.g. Gan et al. 2004; da Silva and de Carvalho 2007; Bombardi and Carvalho 2009). The region is also influenced by the South Atlantic Convergence Zone (SACZ), which is a typical feature of the South American Summer Monsoon. SACZ is characterized by a quasi stationary baroclinic zone oriented in the northwest–southeast direction that extends from the Amazon region to the subtropical South Atlantic Ocean and is associated with cloudiness and heavy precipitation when active (Kodama 1992, 1993; Liebmann et al. 2001; Carvalho et al. 2002, 2004). During an SACZ event, precipitation is generated by the low level converge of moisture due to the northerly flow from the Amazon region and the moisture transport from the South Atlantic subtropical high. Carvalho et al. (2002) observed that most of the extreme events of precipitation over southeastern Brazil, during the austral summer, are associated with the intensification of the SACZ.

Chaves and Nobre (2004) used atmospheric and oceanic general circulation models to study the relationship between the tropical South Atlantic SST anomalies and the seasonal variability of the SACZ during the austral summer (November through February). They verified that warm

SST anomalies over the tropical South Atlantic tend to intensify and move the SACZ northward, while cold SST anomalies tend to weaken this system over land and sea. The intensification and northward migration of the SACZ associated with warm SST anomalies is followed by cooling of surface waters in the SACZ region due to blocking of incoming solar radiation by the increase of cloudiness, characterizing a negative ocean–atmosphere feedback (Chaves and Nobre 2004; De Almeida et al. 2007).

De Almeida et al. (2007) verified that the spatial pattern of SST, that is associated with the ocean–atmosphere feedback, is correlated in time and space with the dominant mode of coupled variability over the South Atlantic Ocean, known as the "South Atlantic Dipole" (SAD). SAD is characterized by a dipole in sea surface temperature anomalies with centers over the tropical and the extratropical South Atlantic (Venegas et al. 1997; Haarsma 2003; Sterl and Hazeleger 2003). According to Venegas et al. (1997), this mode is dominated by interdecadal variability and is related to the strengthening and weakening of the subtropical anticyclone, with the atmosphere leading the ocean by 1–2 months. Haarsma et al. (2005) showed that a simple oceanic mixed layer model can reproduce the SST anomaly patterns when forced with surface winds. However, the authors suggest although the dominant variability is generated by internal atmospheric dynamics, it is still significantly affected by SST variability. Nnamchi et al. (2011) showed that the SAD dipole structure is not an artifact of multivariate linear analyses and that a dipole mode really exists in the South Atlantic Ocean.

Morioka et al. (2011) studied the mechanisms that generate the seasonal evolution of SAD events. They show that the strengthening of the wind stress in the SAD tropical pole increases evaporation and enhances the ocean's surface loss of latent heat and increases the depth of the ocean's mixed layer. A deeper mixed layer is less susceptible to the heating by shortwave radiation resulting, therefore, in negative SST anomalies. In addition, the wind stress is responsible for generating the SST anomalies, but not responsible for destroying them, suggesting that SST changes do not feedback on the atmospheric circulation in a systematic way (Sterl and Hazeleger 2003; Morioka et al. 2011). During the decay phase of SAD, the SST anomalies are damped by entrainment and latent heat (Morioka et al. 2011).

Experiments with global atmospheric models perturbed with SAD spatial pattern of SST anomalies (Haarsma 2003; Robertson et al. 2003) indicate that tropical warm SST anomalies produce a local atmospheric baroclinic response. That is, when the dipole exhibits warm SST anomalies over the tropics, a cyclonic circulation develops at low levels and an anticyclonic circulation develops at upper levels with increased precipitation to the north and suppressed precipitation to the southwest. However, precipitation anomalies in these experiments were largely confined to the ocean (Haarsma 2003; Robertson et al. 2003). Haarsma (2003) showed that the deep baroclinic atmospheric response to the SAD is mainly linear and almost entirely due to the equatorward SST anomaly center. In addition, the baroclinic response is seasonally dependent, stronger during summer and weaker during winter, when the descending branch of the meridional circulation inhibit the development of deep baroclinic response. Haarsma (2003) also observed an equivalent barotropic response over the poleward pole of SAD.

Although the numerical studies of Robertson et al. (2003) and Haarsma (2003) verified a small influence of the South Atlantic SST on precipitation over land, some observational studies have shown significant evidence of a relationship between the South Atlantic SST and precipitation over eastern South America. Muza et al. (2009) observed that negative SST anomalies over the tropical South Atlantic and positive SST anomalies over the subtropical South Atlantic are associated with extreme wet events over southeastern Brazil. Bombardi and Carvalho (2011) observed that SAD is associated with variations in the characteristics of the rainy season over northeastern and eastern Brazil on interannual timescales. They showed that negative SST anomalies over the tropics and positive SST anomalies over the extratropics are associated with increased precipitation during the rainy season over eastern Brazil. Moreover, Nnamchi et al. (2011) showed consistent results during the austral winter, which is the dry season over eastern South America. In addition, Cardoso and Silva Dias (2004) observed that station temperature over southeastern Brazil is also correlated with the South Atlantic SST dipole.

Motivated by these previous works, the objective of this study is to further investigate the role of the South Atlantic SST anomalies on precipitation over eastern South America, during the rainy season and neutral El Niño Southern Oscillation (ENSO) periods. We focus our analyses on neutral ENSO periods to remove the effect of ENSO on precipitation over South America (Grimm et al. 2000, 2007). The study area is located over eastern South America (Fig. 1), a region with approximately 61 % of Brazil's population that accounts for about 73 % of the country's Gross National Product (Source: Brazilian Institute of Geography—IBGE). Therefore, furthering the present understanding of coupled atmosphere–ocean mechanisms that impact the precipitation variability over eastern South America is important for climate monitoring and forecast. This study is organized as follows: Sect. 2 presents the data used in this work. Section 3 discusses the first mode of coupled variability over the South Atlantic

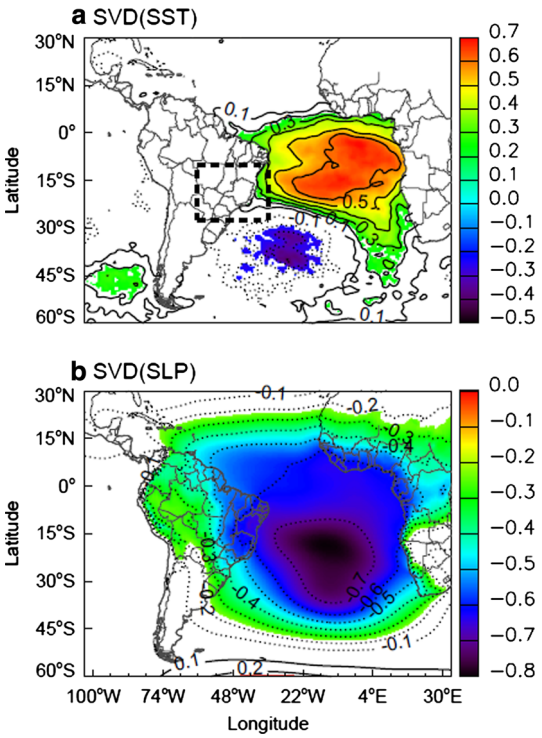

Fig. 1 **a** Correlation between SST anomalies and the $SVD1_{SST}$ time coefficient. **b** correlation between SLP anomalies and the $SVD1_{SLP}$ time coefficient. *Solid lines* show positive correlations and *dotted lines* show negative correlations. Contour interval equal 0.1. *Shade indicates* regions where the correlations are statistically significant at 5 % level. The *dashed line* in (**a**) indicates the region of interest for this study referred as eastern South America

region. The methodology to identify SAD events is described in Sect. 4. Section 5 presents the precipitation and SST pattern that characterize the phenomenon. Some of the mechanisms associated with SAD events are examined in Sect. 6. Section 7 presents the conclusions.

2 Data

This study examines SST data from the NOAA Optimum Interpolation 0.25° Daily Sea Surface Temperature Analysis (Reynolds et al. 2007). This dataset uses satellite measurements (Advanced Very High Resolution Radiometer—AVHRR) and in situ data from ships and buoys and is available from 1982 to the present. In addition, we examined daily gauge precipitation from the Brazilian National Agency of Water (ANA) and 5-day average (pentad) precipitation from the Global Precipitation Climatology Project (GPCP), based on satellite and gauge observations (Xie et al. 2003). GPCP is available from 1979 to the present at 2.5° resolution. We also analyzed daily temperature, horizontal wind, sea level pressure (SLP), geopotential height, and vertically integrated moisture flux from the Modern Era Retrospective-Analysis for Research and Applications (MERRA), with spatial resolution of 0.5° latitude × 0.67° longitude (Rienecker et al. 2011). The period of analysis of this study is from 1982 to 2009. All data were averaged into pentads and anomalies were obtained by removing the linear trend and the annual cycle. Before computing anomalies, the mean annual cycle was smoothed using iterations of a moving average of three points in order to remove noise due to imperfections in the sampling of annual variability (e.g. Hartmann and Michelsen 1989). Due to many missing records in the ANA precipitation dataset, we considered only rain gauge stations with at least 75 % of the records.

In addition, we examined extratropical cyclone tracks over the South Atlantic using the algorithm developed by (Murray and Simmonds 1991a, b). (Reboita et al. 2009) applied the 2008 version of the tracking algorithm to 6-h SLP data from the NCEP-NCAR reanalysis (Kalnay et al. 1996) at 2.5° resolution. Extratropical cyclone tracks were calculated from 1979 to the present for the whole southern hemisphere. This numeric scheme has been used in many studies for the southern hemisphere (Pezza and Ambrizzi 2003; Carvalho et al. 2005; Reboita et al. 2009) and will be summarized as follows.

Candidates to low pressure centers are identified by comparing the values of each grid point to its neighboring grid points. This method seeks grid points at which the laplacian of the SLP is lower than any of the eight surrounding points and greater than a prescribed value. It is important to mention that this method identifies closed lows that are associated with a marked concavity in the pressure surface. These regions characterize a maximum in the Laplacian of the SLP, and hence a maximum in the relative cyclonic geostrophic vorticity. However, a different approach is used to identify open lows, which are common systems in mid-latitudes. Open lows are associated with an inflexion in the pressure surface. Therefore, the point of minimum pressure gradient, which is nearly always associated with a concavity in the pressure field, can be used as a metric to identify open lows. All systems (closed and open lows) identified by this algorithm are tracked from the time of their appearance to their dissipation. To determine the trajectory of the cyclone, the algorithm first estimates the new position and then calculates the probability of associations between the predicted and realized positions. The final match is found with the highest overall probability.

3 The first mode of coupled variability

SAD is a coupled phenomenon and is often defined by performing singular value decomposition (SVD) analysis

of oceanic (SST) and atmospheric (sea level pressure—SLP) components (Venegas et al. 1997; Sterl and Hazeleger 2003). Here we performed SVD analysis of SST and SLP pentad anomalies over the same domain adopted in Nnamchi et al. (2011) [45°S–5°N; 60°W–20°E]. The first mode of coupled variability of the South Atlantic region explains 63 % of the total variance. The spatial pattern of the first SVD of the SST ($SVD1_{SST}$) and SLP ($SVD1_{SLP}$) components is examined by computing correlations between the SVD1 time coefficient and respective SST and SLP anomalies (Fig. 1). The statistical significance was assessed by applying the *t* test at 5 % significance level. All datasets exhibit large autocorrelation. Thus, the degree of freedom was estimated as the effective number of degrees of freedom (Neff) according to Wilks (2006) (Eq. 1).

$$Neff = N \cdot \left(\frac{1-\rho}{1+\rho}\right) \quad (1)$$

where N is the number of records (2,044 pentads) and ρ is the lag 1 autocorrelation. The same approach was used to assess statistical significance in all analyses of this paper.

The $SVD1_{(SST)}$ pattern characterizes a dipole with opposite anomalies between the tropics and extratropics (Fig. 1a). It is noticeable, however, that the region with statistically significant correlations (at 5 % significant level) ranging from −0.1 to −0.4 is confined to a small area in midlatitudes around 45°S and 35°W. In contrast, correlations as high as 0.7 and statistically significant regions are observed in a large area over the tropics. The relatively lower correlation in the extratropical pole of the $SVD1_{(SST)}$ is consistent with previous studies (Venegas et al. 1997; Sterl and Hazeleger 2003; Bombardi and Carvalho 2011). This issue will be examined in detail in Sect. 5. The $SVD1_{(SLP)}$ component characterizes a large monopole that extends over most of the tropical Atlantic and extratropical South Atlantic (Fig. 1b). The spatial patterns of $SVD1_{(SST)}$ and $SVD1_{(SLP)}$ resemble the SAD spatial pattern as defined in several previous studies (Venegas et al. 1997; Haarsma 2003; Sterl and Hazeleger 2003; Nnamchi et al. 2011). It is worth noticing that the $SVD1_{(SST)}$ and $SVD1_{(SLP)}$ modes were obtained with relatively shorter period of data and higher temporal resolution comparatively to the respective modes discussed in Venegas et al. (1997). Consequently, the SVD1 modes calculated here exhibit variations on shorter time scales that have not been shown before. Nonetheless, our results are consistent with the large majority of previous studies and the SVD-1 mode will be hereafter referred to as SAD. The following analysis will focus on the $SVD1_{(SST)}$ component (henceforth SVD-1).

The SVD-1 time variability was evaluated using wavelet power spectrum analysis (e.g. Torrence and Compo 1998). The wavelet analysis provides information about the spectral variance over time. High statistically significant (at 5 % significance level) amplitudes of the power spectrum are observed around 500–1,000 days (1.4–2.8 years), 1,825 days (5 years) during the 1990s, and below 100 days throughout the period of study (Fig. 2). These results are consistent with (Trzaska et al. 2007; Bombardi and Carvalho 2011) and suggest the importance of the intraseasonal (20–100 days) to interannual (1–3 years) variability of SAD during the period of analysis.

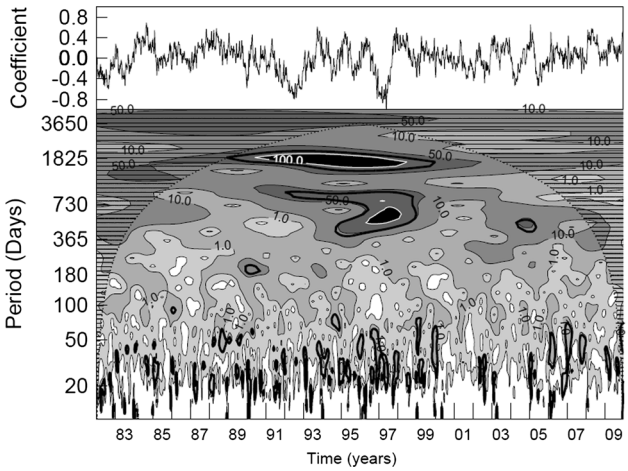

Fig. 2 Wavelet power spectrum of the SVD-1 time coefficient. The '*y*' axis is the period (in pentads). The *shaded contours* are the normalized variances of 5, 10, 20, 50, 100, 200, 350, and 730. The '*x*' axis is time (in years). *Striped regions* indicate the cone of influence where the edge effects become important. The *solid thick line* presents periods when the power spectrum is statistically significant at 95 % level (see Torrence and Compo 1998)

4 Identification of SAD events

Recent studies have shown evidence that the tropical Pacific SST is influenced by the tropical Atlantic Ocean. Kayano et al. (2011) observed that persisted SST anomalies in the tropical Atlantic Ocean can be identified 5–6 months prior to ENSO events. In addition, Bombardi and Carvalho (2011) observed significant correlations between the SAD and ENSO indices and showed that SAD leads ENSO by 5–12 months. Likewise, Nnamchi et al. (2011) showed that SAD leads ENSO by 7–8 months. However, Rodrigues et al. (2011) found that El Niño events also play an important role on SST anomalies over tropical and extratropical South Atlantic. According to the authors, the response of the Atlantic SST anomalies to weak and short El Niño events is opposite to the response to strong and long El Niño events.

ENSO is the main mode of coupled variability on interannual timescales that impacts South America (Grimm et al. 2000, 2007). Taschetto and Wainer (2008) suggested

that the impact of the South Atlantic subtropical–extratropical SST anomalies on the convection over tropical South America is counteracted by the effect of the ENSO. To remove the effect of ENSO on precipitation over South America, we focus our analysis on periods when ENSO was considered neutral according to the Climate Prediction Center of the National Oceanic and Atmospheric Administration (NOAA). More information can be found at http://www.cpc.ncep.noaa.gov/products/analysis_monitoring/ensostuff/ensoyears_1971-2000_climo.shtml.

SAD events of interest were selected during neutral ENSO conditions and based on the variability of SVD-1 time coefficient as follows. The SVD1-1 index was smoothed with a three-point moving average. Positive SAD events were defined as the period when the smoothed SVD-1 time coefficient was above the SVD-1 75th percentile for at least three consecutive pentads. Likewise, negative SAD events were selected when the smoothed SVD-1 time coefficient was below the SVD-1 25th percentile. Figure 3 shows the SVD-1 time coefficient and the selected events. We examined SAD events that occurred from September to April, the rainy season over eastern South America (Gan et al. 2004; da Silva and de Carvalho 2007; Bombardi and Carvalho 2009) and are separated from ENSO events by at least 1 month (167 pentads for negative SVD-1 and 110 pentads for positive SVD-1).

Intense negative SAD events were observed prior the strong El Niños of 1982/1983 and 1997/1998, whereas intense positive SAD events were observed before the intense La Niñas of 1988/1989 and 1998/1999 (Fig. 3). These results are consistent with Bombardi and Carvalho (2011) and Kayano et al. (2011, 2012). Although ENSO and SAD seem to interact (Rodrigues et al. 2011; Kayano et al. 2012), the relationship is not systematic. For example, a very intense negative SAD event started during the El Niño 1991/1992, while positive SAD was observed during the El Niño events of 2004/2005 and 2009/2010 (Fig. 3). Kayano et al. (2012) showed that correlations between SAD and ENSO are affected by decadal variability, with ENSO leading SAD from 1940 to 1970 and SAD leading ENSO from 1970 to 2000.

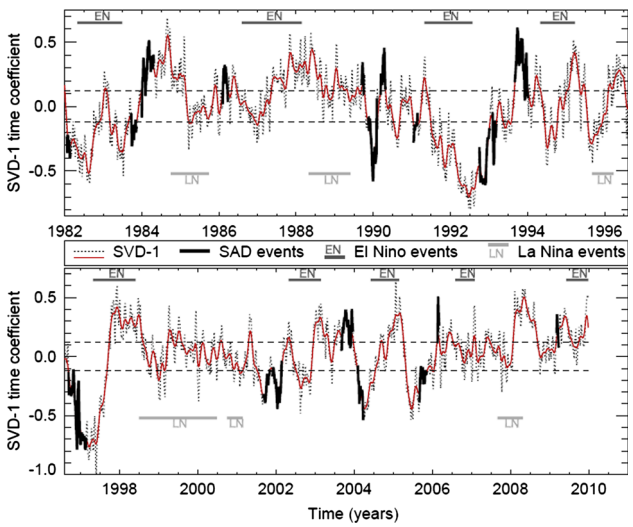

Fig. 3 Normalized SVD-1 time coefficient and selected SAD events. The *red line* is the smoothed SVD-1 index using a three-point moving average. The *dashed lines* represent the 25 and 75 % percentile of the SVD-1 index. SAD events were selected during non-ENSO periods. The duration of ENSO events are represented by *horizontal bars*. SAD events are separated from ENSO events from at least 1 month. SAD events are separated from each other by at least 5 pentads

5 Characterizations of SAD events

Negative SAD events are characterized by negative SST anomalies over the tropical South Atlantic and along the African coast and positive SST anomalies over the western and central extratropical South Atlantic (Fig. 4a). This pattern is associated with positive precipitation anomalies over eastern South America. Carvalho et al. (2002, 2004) studied the behavior of the SACZ considering different categories that include intense, weak, oceanic and continental SACZ events. The precipitation anomalies associated with the negative phase of SAD resemble the intense-oceanic SACZ category, which indicates that the South Atlantic SST anomalies play a significant role in the variability of modulating the SACZ and consequently the variability of precipitation over eastern South America.

During positive SAD events, we observe positive SST anomalies over the tropical South Atlantic related to decreased precipitation over eastern South America and increased precipitation over north–northeastern Brazil. The extratropical pole is more evident during negative events, which explains why the $SVD1_{(SST)}$ exhibits a weaker extratropical pole compared to the tropical pole (Figs. 1a, 4d). In addition, Nnamchi et al. (2011) showed that during the austral winter, negative SAD events are associated with increased precipitation in parts of central South America, eastern South America, and northern Argentina, and decreased precipitation over other tropical regions such as northeastern Brazil and western Africa. Although the work of Nnamchi et al. (2011) focused on the dry season, our results suggest that SAD events impact precipitation over tropical South America during the wet season as well. Previous studies have also shown that warm SST anomalies over the tropical South Atlantic are associated with wet years over northeastern Brazil on interannual timescales (Moura and Shukla 1981; Uvo et al. 1998; Saravanan and Chang 2000).

Figure 5 shows composites of precipitation anomalies for each phase of SAD events. During negative events,

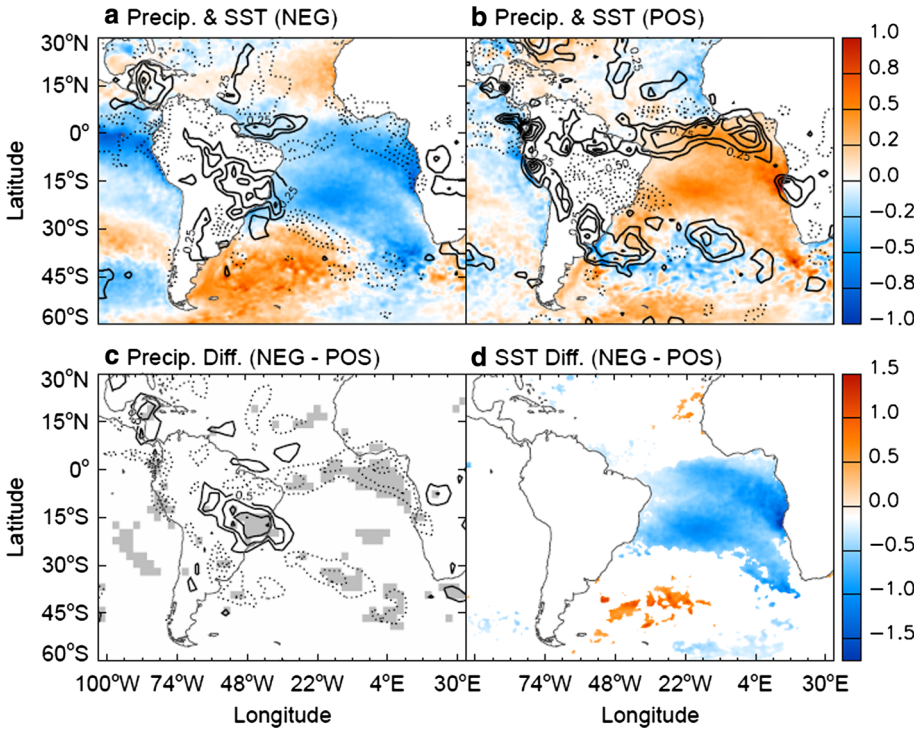

Fig. 4 Composites of SST anomalies (*shade*) and precipitation (*contour*) during **a** negative SAD events (NEG); **b** positive SAD events (POS). Difference between composites of SAD events (negative minus positive) for **c** precipitation and **d** SST. *Shading* in **c** and **d** indicate regions where the difference is statistically significant at 5 % level according to the z-test of the difference of means. Contour interval equal 0.25 mm day^{-1} in (**a**) and (**b**) and equal 0.5 mm day^{-1} in (**c**)

increased precipitation is observed over the eastern South America, while negative precipitation anomalies are observed over southern Brazil and in a few stations over northeast Brazil (Fig. 5a). Positive SAD events are associated with the opposite pattern of precipitation: negative anomalies over eastern South America and positive anomalies over the subtropics (Fig. 5b). Statistically significant precipitation differences between distinct SAD phases are consistent only over eastern South America, indicating that positive SST anomalies over the tropical Atlantic (positive SAD events) are associated with decreased precipitation over eastern South America (Fig. 5c).

6 Mechanisms of SAD events

To identify existing mechanisms relating SAD to precipitation variability over Brazil, we examined the vertically integrated moisture transport during SAD events. During negative SAD events we observe cyclonic anomalies over the extratropical Pacific, anticyclonic anomalies over the extratropical Atlantic, and cyclonic anomalies over southeastern Brazil (Fig. 6a). These results are similar to the wave pattern observed by Liebmann et al. (1999) related to sub-monthly (2–30 days) variations of the SACZ. Liebmann et al. (2004) found that intense precipitation over the SACZ region is related to the propagation of mid-latitude disturbances that originate in the mid-latitude Pacific and turn equatorward as they cross the Andes. These waves weaken the southward moisture flux east of the Andes (Liebmann et al. 2004). On interannual timescales, Doyle and Barros (2002) verified that enhanced convection over the SACZ region is associated with weak southward moisture flux. Carvalho et al. (2010) also identified similar patterns of moisture transport associated with enhanced SACZ on intraseasonal (10–100 days) timescales. Likewise, we show that the positive precipitation anomalies during negative SAD events (Fig. 5a) are associated with a northward anomalous moisture transport east of the Andes (Fig. 6a), which indicates the weakening of the South American low level jet (Marengo et al. 2004). When the LLJ is strong, the moisture flux is strongest toward southeast South America (northern Argentina, Uruguay, and southern Brazil) increasing precipitation in these regions. When the LLJ is weak, the moisture flux intensifies toward southeast Brazil, increasing precipitation in the SACZ region (Doyle and Barros 2002; Liebmann et al. 2004; Marengo et al. 2004). In addition, the westerly anomalies in the moisture transport around 15°S, associated with the anomalous cyclonic circulation, have been largely related to the enhancement of precipitation and convection in the SACZ (Carvalho et al. 2004).

The anomalous cyclonic circulation over eastern South America (Fig. 6a) is also similar to the low-level circulation pattern on interannual timescales discussed in Robertson and Mechoso (2000). This pattern was related to negative SST anomalies over the tropical Atlantic and

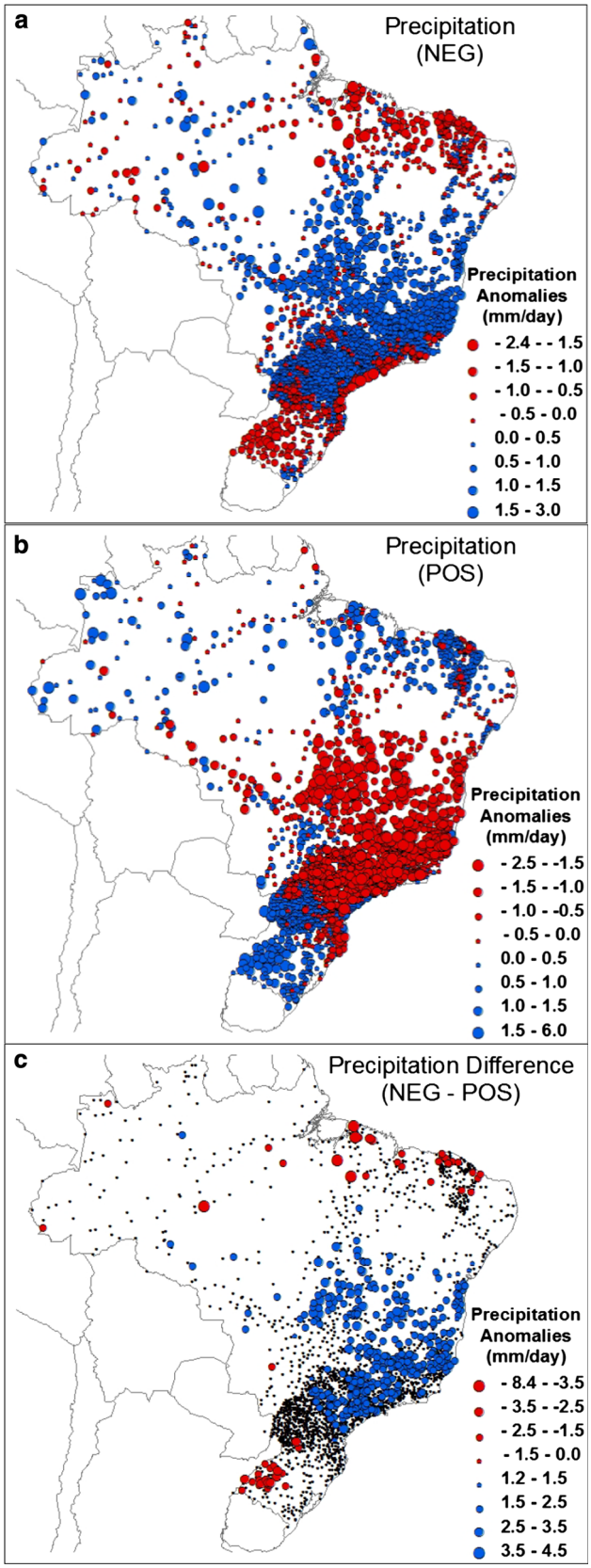

◀ **Fig. 5** **a** Precipitation composite during negative SAD events (NEG); **b** precipitation composite during positive SAD events (POS); and **c** Precipitation difference between positive and negative SAD events (negative minus positive). Precipitation difference values in (**c**) are shown only for station where the difference is statistically significant at 5 % level according to the z-test of the difference of means. *Black dots* in (**c**) represent the location of all available stations

positive SST anomalies over the extratropical South Atlantic (Robertson and Mechoso 2000).

During positive SAD events, we observe anomalous anticyclonic circulation over southeast Brazil and over the subtropical Pacific Ocean (Fig. 6b). Muza et al. (2009) studied the occurrence of extreme wet and dry events over southeast Brazil on intraseasonal timescales. The anomalous moisture flux pattern during positive SAD phase (Fig. 6b) is very similar to the low level circulation anomalies associated with dry events in that region observed by Muza et al. (2009) (see their Fig. 8b).

It has been previously documented that the weakening and strengthening of the low and upper level winds on intraseasonal timescales, over eastern South America, are related to the active and break phases of the South American Monsoon and the organization and maintenance of the SACZ (Carvalho 2002; Herdies 2002; Jones and Carvalho 2002). According to (Ma et al. 2011), the increase in precipitation over the continental SACZ region can be largely explained by advection of the moist static energy. The anomalous cyclonic circulation strengthens the westerly winds over eastern South America and reduces the advection of low moist static energy air from the Atlantic Ocean, favoring deep convection and precipitation. On the other hand, the strengthening of the easterly winds (or weakening of the westerly winds) increases the influx of air with low moist static energy and suppresses deep convection.

Figure 6c, d displays moisture flux divergence composites for both phases of SAD. The moisture flux divergence was calculated from daily mean values of the zonal and meridional components of the vertically integrated moisture flux. Due to the high spatial resolution, the vertically integrated moisture flux exhibits large spatial variability. This spatial variability largely affects the calculation of finite differences. For this reason, we smoothed the vertically moisture flux prior to the calculation of the divergence. The tropical Atlantic exhibits anomalous divergence of the integrated moisture flux during negative SAD events (Fig. 6c). Anomalous divergence is also observed east of the Andes and central Brazil, consistent with the weakening of the low level jet east of the Andes (Fig. 6a). We observe a weak and not

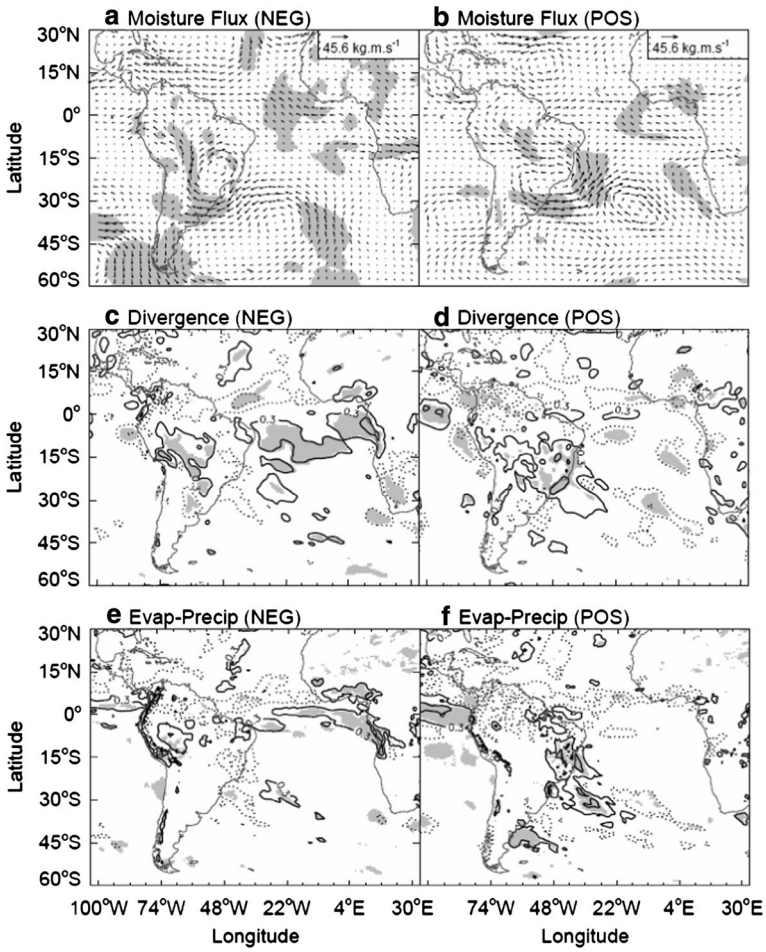

Fig. 6 Vertically integrated moisture flux anomalies during **a** SAD negative events (NEG) and **b** SAD positive events (POS). Divergence anomalies of the vertically integrated moisture flux during **c** SAD negative events and **d** SAD positive events. Evaporation minus precipitation during **e** SAD negative events and **f** SAD positive events. *Shading* represents regions where the anomalies are statistically significant at 5 % level according to a t test. Contour interval in **c**–**f** equal −0.9, −0.3, 0.3, and 0.9 mm day^{-1}

statistically significant anomalous convergence of moisture over eastern South America (Fig. 6c). The transient characteristic of the SAZC increases the variability of the moisture flux divergence which results in low statistical significance of the composite over eastern South America. Moisture divergence increases over eastern South America and adjacent ocean during positive SAD events (Fig. 6d) indicating that positive SAD events are associated with below normal SACZ activity.

We also calculated composites of evaporation minus precipitation (E-P) in order to compare with the composites of moisture flux divergence. We observe that there are large differences between the fields of moisture flux divergence and the fields of evaporation minus precipitation (Fig. 6c–f), especially over the tropical Atlantic Ocean. Trenberth et al. (2011) showed that the precipitation and evaporation produced by reanalyses over the ocean are unreliable. The authors also pointed out problems in precipitation and evaporation from the MERRA reanalysis over southern Amazon and central South America during the summer. However, MERRA representation of evaporation minus precipitation over eastern South America is reasonable (Trenberth et al. 2011) and the results from the moisture flux divergence are consistent with the results from the E-P analyses in that region (Fig. 6c–f). Therefore, these results provide additional evidence that SAD positive events favor evaporation over precipitation in eastern South America.

The upper level wind patterns are very distinct in each phase of SAD (Fig. 7). The overall wind magnitude is stronger during positive SAD events (Fig. 7a) than during negative SAD events (Fig. 7b). Negative SAD events are associated with an anomalous anticyclonic circulation over tropical South America and subtropical South Atlantic. As a consequence, the upper level westerlies strengthen around 25°S and the upper level westerlies weaken around 40°S (Fig. 7c). Liebmann et al. (2004) showed similar pattern of upper level wind anomalies associated with intense precipitation events in the SACZ region. On the other hand, positive SAD events are related to anomalous anticyclonic circulation over the tropical South Atlantic and an intensification of the subtropical jet stream (Fig. 7d). These results suggest that the ocean–atmosphere coupling during SAD events extends throughout the troposphere with potential impacts to the storm tracks and the propagation of extratropical cyclones near the east coast of South America.

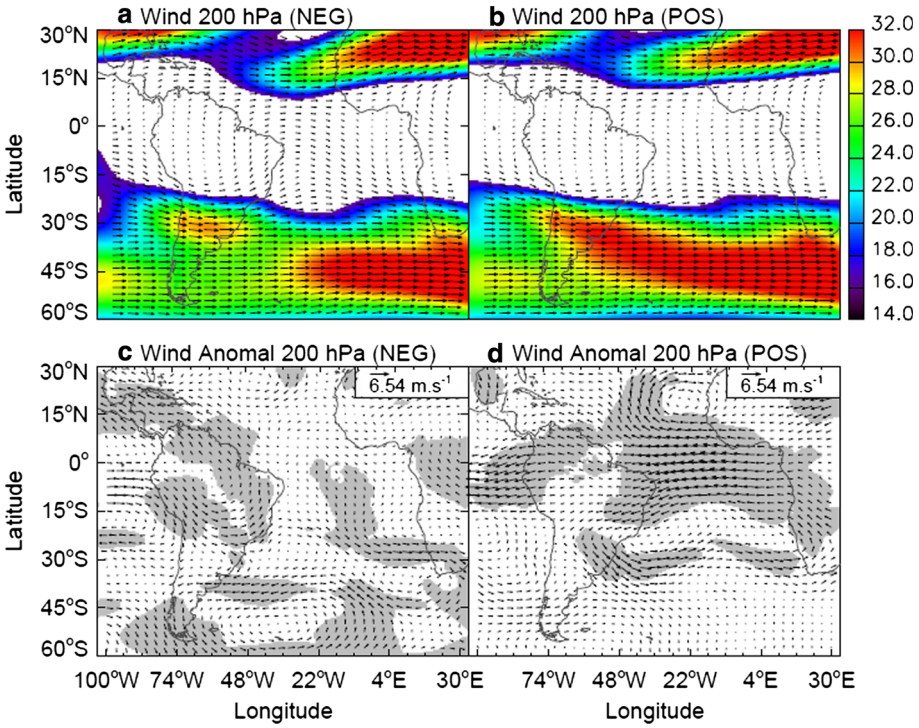

Fig. 7 Wind at 200 hPa (*vector*) and magnitude (*shade*) during **a** SAD negative events (NEG) and **b** SAD positive events (POS). Wind anomalies at 200 hPa (vector) during **c** SAD negative events (NEG) and **d** SAD positive events (POS). Shading in **a** and **b** represents wind magnitude above 16 m s^{-1}. Shading in **c** and **d** represents regions where the anomalies are statistically significant at 5 % level according to a t-test

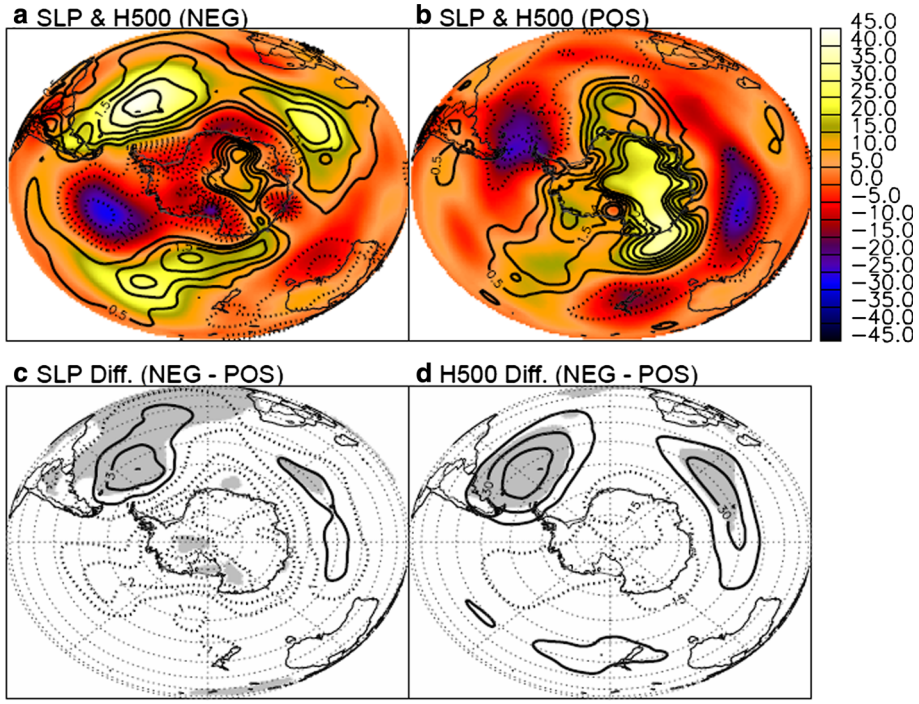

Fig. 8 SLP (*contour*) and geopotential height at 500 hPa (*shade*) during **a** negative SAD events (NEG) and **b** positive SAD events (POS). Difference between negative and positive SAD events composites of **c** SLP and **d** geopotential height at 500 hPa. Shading in **c** and **d** indicate regions where the difference is statistically significant at 5 % level according to the z-test of the difference of means. Contour interval equal 0.5 hPa in **a** and **b**, equal 1 hPa in (**c**), and equal 15 m in (**d**)

During SAD negative events, negative SLP and 500 hPa geopotential anomalies are observed to the west of South America in midlatitudes, while positive SLP and geopotential anomalies are observed over the western extratropical South Atlantic, extending towards the Indian Ocean (Fig. 8a). These results are consistent with the climatology of persistent positive anomalies of 500-hPa geopotential height for the austral summer (Renwick 2005). Conversely, positive SAD events show negative SLP and geopotential anomalies over the western South Atlantic and positive anomalies to the west of South America and over the eastern South Atlantic (Fig. 8b). Statistically significant differences of SLP and geopotential height are observed over the western extratropical South Atlantic (Fig. 8c, d).

Blocking events in the southern hemisphere are rare over the western extratropical South Atlantic (e.g. Sinclair 1996). However, Sinclair (1996) identified summer anticyclone formation maxima in localized regions southeast of major mountain barriers, such as the Andes. Moreover, the intensification of anticyclones tend to occur downstream and slightly poleward from the corresponding formation locations. Intensifying anticyclones are most frequent in western ocean basins such as southeast South America (Sinclair 1996). During SAD negative events, the warm waters of the western extratropical South Atlantic appear associated with the intensification of anticyclones that form southeast of the Andes and extend over the west extratropical Atlantic basin (Fig. 8c). The enhanced subsidence inhibits cloud formation and increase incoming solar radiation over the ocean surface, which favors the warming of the extratropical South Atlantic. In addition, the midlatitude anticyclonic anomaly during negative SAD events (Fig. 8a, c) also affect low-tropospheric circulation in the South Atlantic basin by increasing the southerly winds near the west coast of Africa and the northerly winds near the east coast of South America. These features are coherent with the SST anomalous patterns observed during SAD phases and provide important insights about the ocean–atmosphere coupled mechanisms responsible for the existence and maintenance of the SAD mode.

To verify the relationship between the storm tracks and SAD, we compare the statistics of the extratropical cyclone tracks during SAD events. We selected the cyclones with at least 24 h of duration that initiated in latitudes south of 15°S over the ocean and south of 25°S over South America, considering that southern South America is an active region for cyclogenesis (Gan and Rao 1991; Simmonds and Keay 2000; Hoskins and Hodges 2005; Reboita et al. 2010). The initial position of the cyclones (cyclogenesis) and their trajectories (density tracks) were examined with a method known as spherical kernel (Hodges 1996). This method uses the location tracks of cyclones to create a map of density under the assumption that a cyclone impacts a certain area with a given radius (or bandwidth). For example, by superposing the areas of influence of the initial position of each cyclone, one can estimate a density map for cyclogenesis. The density track analysis takes into account the trajectory of the cyclones and, therefore, requires a careful interpretation, given that the tracks of a single cyclone are not independent. The calculation of track density is different from the calculation of cyclogenesis density. The track density is not simply the kernel estimate using all points of each cyclone event. The track density is calculated locally based on a stationary observer. For each grid point, we find the nearest track point of each cyclone event, using the great circle distance measure. Then, we sum the kernels only at that grid point and we repeat this process for the other grid points. This way, the track density is not biased by the number of track points of each cyclone event, given that only one location is considered for each cyclone. In this paper we used the linear case ($m = 1$) of the power function proposed by Hodges (1996). In addition, we used a fixed smoothing parameter ($Cn = 94.5$) defined by the cross-validation function, also proposed by Hodges (1996).

Climatologies of cyclogenesis over South America show three main regions of cyclogenesis for the austral summer (Sinclair 1996; Hoskins and Hodges 2005; Reboita et al. 2010). The strongest one is located just off the South American east coast around 42°S–47°S. Two secondary maximums are observed over Uruguay (around 32°S) and offshore southeast Brazil (around 26°S). During negative SAD events, the maximum cyclogenesis is observed offshore of southeast Brazil coast (Fig. 8a). On the other hand, the region of major cyclogenesis during positive SAD events is observed over Uruguay and adjacent ocean (Fig. 10b). Reboita (2008) verified that cyclones generated over the Uruguay region tend to be associated with upper level troughs, with little influence from SST and latent heat fluxes. In addition, cyclones generated offshore of southeastern Brazil are strongly related to SST and latent heath fluxes (Reboita 2008). Therefore, the two phases of SAD are associated with a different region of maximum cyclogenesis.

The tracks of the cyclones generated over the main regions of cyclogenesis over Uruguay and offshore southeast Brazil are shown in Fig. 9c and d. During negative SAD events, a higher number of cyclones are observed over the ocean near southeast Brazil, whereas during positive SAD events (Fig. 9d), cyclones are more concentrated over Uruguay and adjacent ocean. However, looking at individual tracks might be misleading. Therefore, we also computed the cyclone track density for each phase of SAD. During negative SAD events, a high density of cyclone trajectories are observed in the region with warm SST anomalies around 40°S–50°S, moving northward over the ocean along the South American east coast from the coast of Uruguay toward southeast Brazil. Then, the systems move southeastward along the southern edge of the SACZ region (Fig. 9e), consistent with the findings of Hoskins and Hodges (2005). During SAD positive events, the cyclone tracks are much more restrict to latitudes around 40°S (Fig. 9f). The cyclogenesis and density track differences clearly show a higher frequency of cyclones near southeast Brazil during SAD negative events in comparison with SAD positive events (Fig. 9g, h), which is probably the main cause for the increased precipitation over central–eastern South America during negative SAD events. During negative SAD events the storm track would move further north than during positive SAD events. The SACZ is the most important feature during summer that

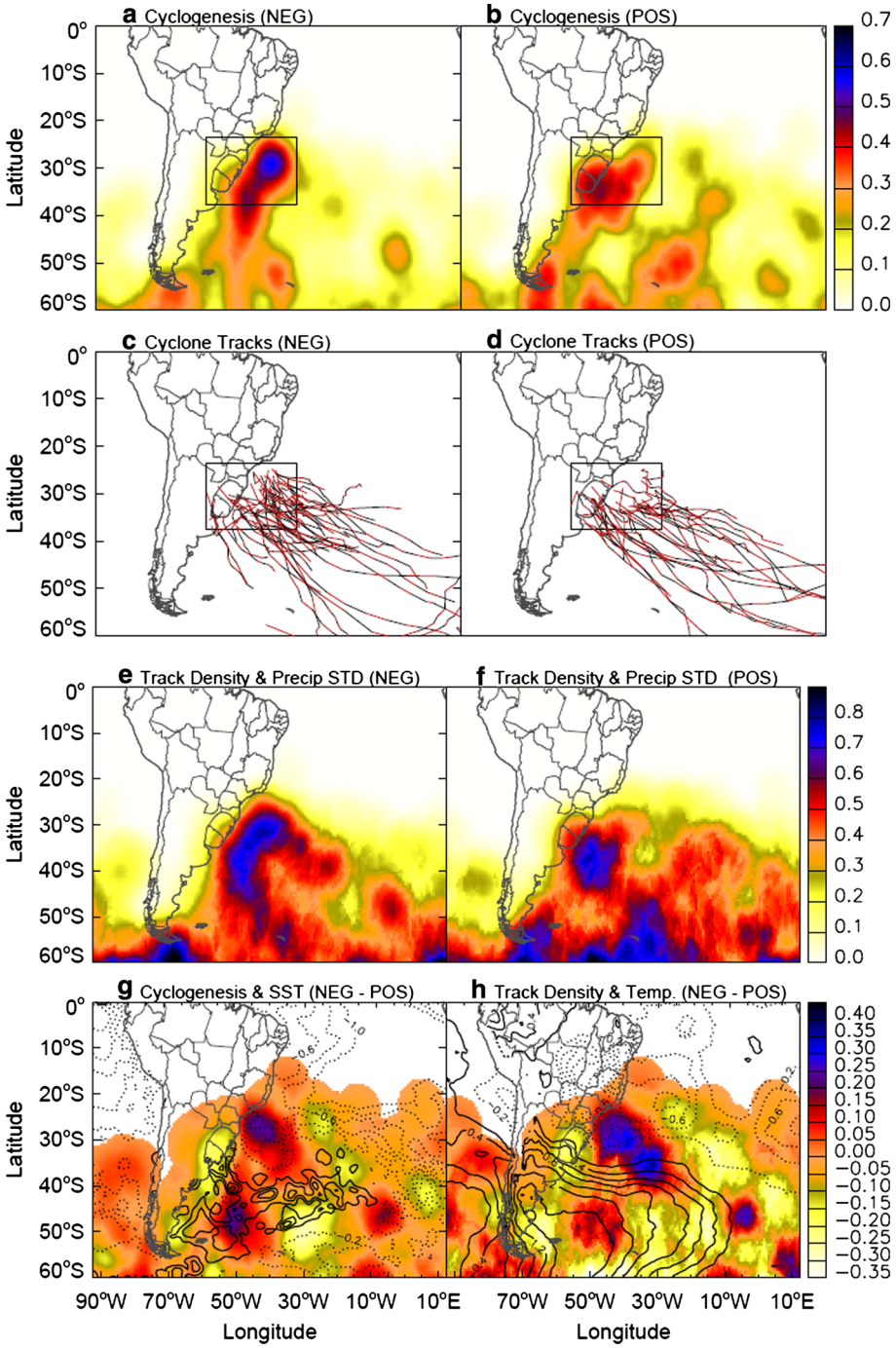

Fig. 9 Cyclogenesis density (number of cyclones by square radian per day) during **a** negative SAD events (NEG) and **b** positive SAD events (POS). Cyclone tracks of cyclones originated over the region of maximum cyclogenesis during **c** negative SAD events and **d** positive SAD events. Cyclone density track (number of cyclones by square radian per day) during **e** negative SAD events and **f** positive SAD events. Difference between negative and positive SAD events composites of **g** cyclogenesis (*shaded*) and mean SST (*contour*) and **h** cyclone density track (*shaded*) and mean temperature at 850 hPa (*contour*). *Solid lines* show positive values and *dotted lines* show negative values. Contour interval equal 0.2 K in **g** and **h**

modulates precipitation over eastern coast of Brazil (Liebmann et al. 2001; Carvalho et al. 2002, 2004). The transient variability of the SACZ on subseasonal time scales is associated with the propagation of the extratropical cyclones over the Atlantic (e.g. Liebmann et al. 1999). The intensification of daily precipitation over the southeast coast of Brazil depends on the extent and intensity of the SACZ as well as on its proximity of the continent (Carvalho et al. 2004). This study shows that these features can be largely associated with changes in SAD. The differences in the mean fields of SST (Fig. 9g) and temperature at 850 hPa (Fig. 9h) show negative values over the ocean near southeast Brazil, which agrees with (Chaves and Nobre 2004) that propose that the SACZ cools SST by radiation feedback mechanisms.

To further verify the importance of the synoptic scale during SAD events, we analyze the daily evolution of meridional wind at 200 hPa, filtered on 3–10 days (Figs. 10, 11). For this purpose, daily precipitation anomalies were spatially averaged over eastern South America

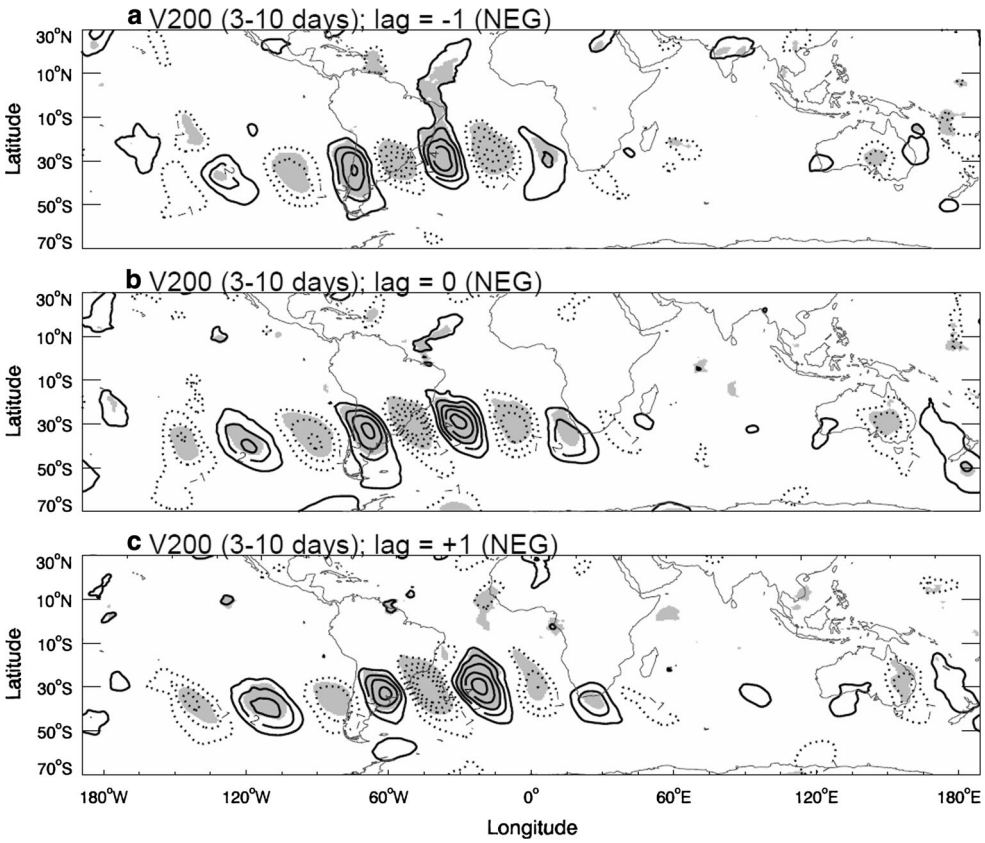

Fig. 10 Daily Lag composite of meridional wind at 200 hPa, filtered on 3–10 days, for rainy days (above 75th percentile) during negative SAD events (NEG). Contour interval equal 1 m s^{-1} going from −5 to 5 m s^{-1}. *Shading* indicates regions where the anomalies are statistically significant at 5 % level according to the t-test

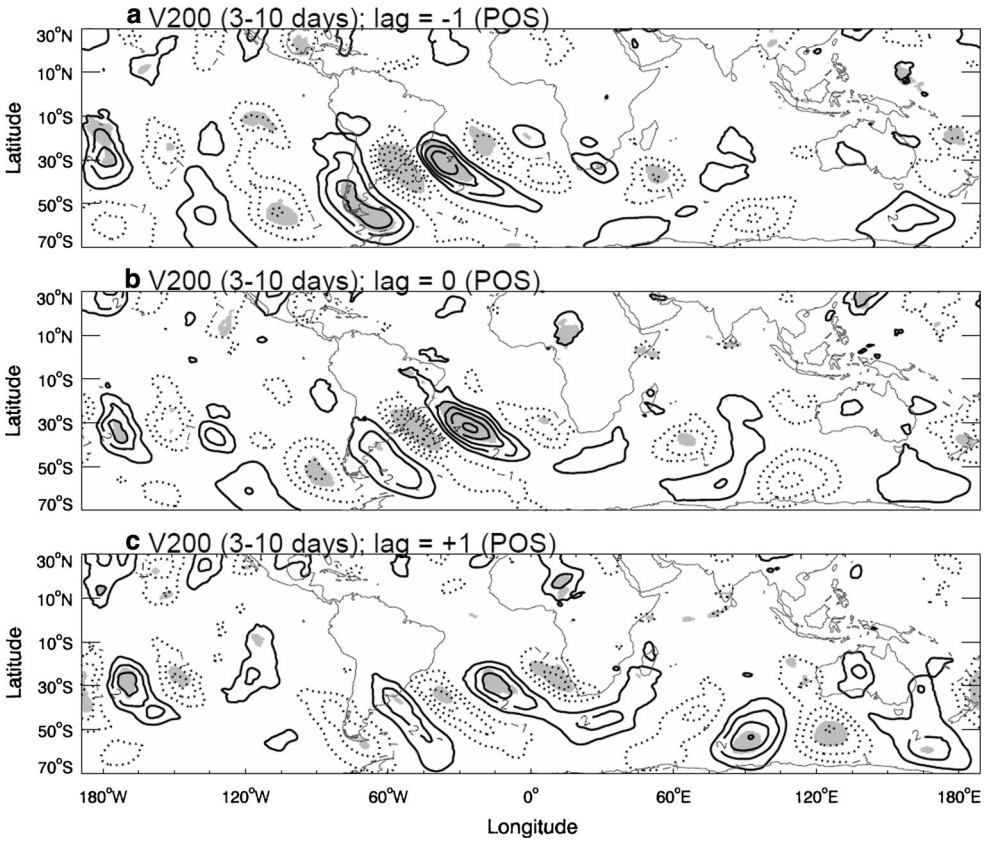

Fig. 11 Daily Lag composite of meridional wind at 200 hPa, filtered on 3–10 days, for rainy days (above 75th percentile) during positive SAD events (POS). Contour interval equal 1 m s^{-1} going from −5 to 5 m s^{-1}. *Shading* indicates regions where the anomalies are statistically significant at 5 % level according to the t-test

(Fig. 1). Only the days with precipitation anomalies greater than zero were selected and the precipitation threshold that represents the 75th percentile was calculated. Lag composites were constructed only for days with precipitation above the 75th percentile that occurred during SAD events. We observe that during negative SAD events, precipitation is associated with a zonal wave extending between 30°S and 40°S (Fig. 10) with an almost east–west (or zonal) orientation. The zonal structure of the wave pattern favors anticyclonic circulation east of the Andes and cyclonic circulation over the east coast of Brazil, consistent with the intensification of the SACZ (Carvalho et al. 2004; Liebmann et al. 2004). These features are associated with the equatorward displacement of the cyclones and consequent increase in precipitation over eastern South America. In contrast, precipitation during positive SAD events is associated with a wave pattern with a southwest–northeast orientation that resembles the wave patterns discussed in Liebmann et al. (2004) (Fig. 11). In this case, the systems are less likely to cross the Andes topography, thus reducing the probability of intensifying anticyclogenesis in midlatitudes.

The selection of SAD events only during neutral ENSO periods is very restrictive. Therefore, we investigate the distribution of precipitation expanding the period of SAD events as follows. SAD events as defined in Fig. 3 (Fig. 12a); SAD negative (SVD-1 below 25th percentile) and SAD positive (SVD-1 above 75th percentile) for the entire period regardless of ENSO events (Fig. 12b); SAD negative and SAD positive only during El Niño events (Fig. 12c); and SAD negative and SAD positive only during La Niña events. The period of interest is from November to March and only pentads with precipitation greater than zero were considered. Precipitation distributions during neutral ENSO events (Fig. 12a) are very similar to that of the entire period (Fig. 12b). In both cases, SAD negative events show a significant increase of the 75th percentile of precipitation in comparison with SAD positive events at 5 % level. The significance of the difference in proportions is given by the sign test for difference in locations considering the continuity adjustment presented in (Anderson and Finn 1996). These results suggest that the increase in precipitation over eastern South America holds true for the entire period. When we consider only El Niño events, we observe a significant increase in the median of precipitation during SAD positive in comparison with negative SAD (Fig. 12c). On the other hand, when considering only La Niña events, there is a significant increase in the median of precipitation during negative SAD in comparison with positive SAD (Fig. 12d). These results indicate the importance of separating the influence of ENSO when investigating the importance of the South Atlantic for the climate over South America.

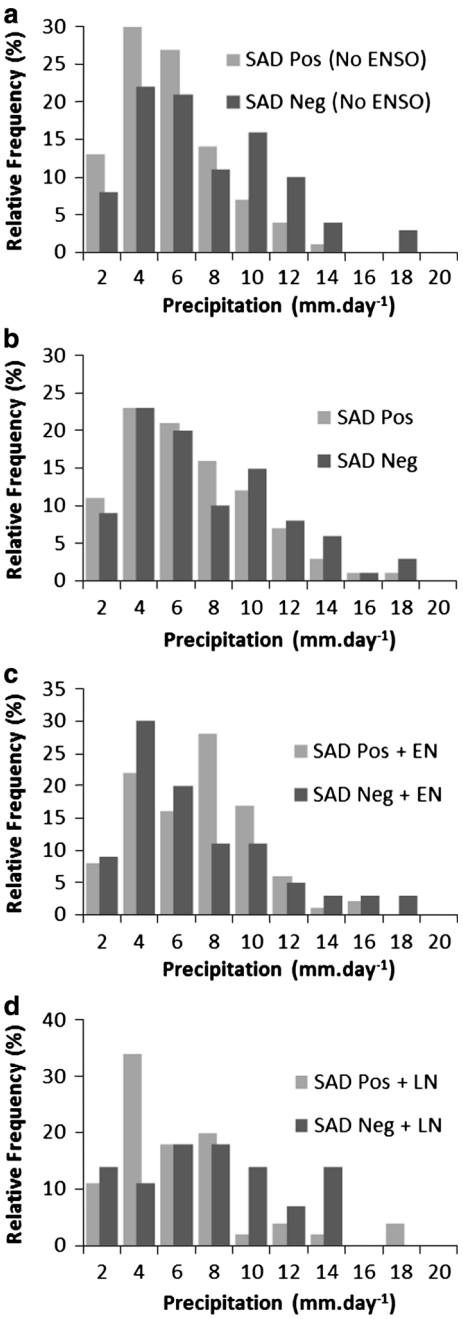

Fig. 12 Relative frequency of precipitation (GPCP) during November–February averaged over 22.5S–12.5S and 50 W–40 W. **a** SAD events as defined in Fig. 3. **b** SAD negative (SVD-1 below 25th percentile) and SAD positive (SVD-1 above 75th percentile) regardless of ENSO events. **c** SAD negative and SAD positive only during El Niño (EN) events. **d** SAD negative and SAD positive only during La Niña (LN) events

7 Conclusions

The present study showed important relationships between SAD and precipitation over Brazil. This work has focused on periods when ENSO was considered neutral. Our results suggest that SAD ocean–atmosphere coupling is such that

the changes in the South Atlantic SST are associated with variations in the position and intensity of the midlatitudes anticyclones. Therefore, SAD plays a significant role in the organization of the SACZ by influencing the position and movement of extratropical cyclones.

Negative SAD events are characterized by negative SST anomalies over the tropical South Atlantic, positive SST anomalies over the extratropical South Atlantic, and positive SLP anomalies over the whole South Atlantic. Cyclonic moisture transport over southeastern Brazil, with westerly moisture flow is associated with increased precipitation over eastern South America. These features are observed along with a high density of cyclogenesis near the southeast coast of Brazil. The cyclones tend to move northward and then southeastward along the region of influence of the oceanic SACZ. Therefore, the increased precipitation over eastern South America, during negative SAD events, seems to be associated with the organization of the SACZ and respective extratropical cyclones. Anticyclogenesis east of the Andes and the anticyclone intensification over western extratropical South Atlantic seem to be related to the generation of positive SST anomalies as well as the northward displacement of the transients.

In contrast, SAD positive events are characterized by positive SST anomalies over the tropical South Atlantic, weak negative anomalies over the extratropical South Atlantic, and negative SLP anomalies over the whole South Atlantic. Our analyses show an intensification of the subtropical jet over subtropical South America and low frequency of extratropical cyclones near southeastern Brazil, indicating a southward displacement of the storm tracks in comparison with negative SAD events. Consequently, dry conditions are observed over eastern South America.

Precipitation events during negative SAD events are associated with a more zonal propagation of synoptic disturbances in comparison with positive SAD events. Our results suggest that this zonal wave pattern would intensify the anticyclones east of the Andes. These anticyclones are associated with the warm extratropical South Atlantic Ocean and are likely the most important atmospheric feature to force the displacement of extratropical cyclones northward. The combined interplay of the formation and trajectory of cyclones and the resulting organization of SACZ near the coast result in increased precipitation over southeastern and central Brazil. Synoptic disturbances during precipitation events occurring in positive SAD phases do not show strong anticyclonic anomalies in subtropical latitudes east of the Andes and develop in relatively cold waters of the extratropical South Atlantic. Cyclones observed along with these synoptic features have trajectories away from the east-coast of Brazil. This analysis provides additional evidence that SAD coupled mechanisms affect the position of the SACZ and total daily precipitation over the wet season in these regions. Therefore, the monitoring of the South Atlantic Ocean variability on intraseasonal to interannual time scales has significant impact for climate prediction of South America.

Acknowledgments We thank the anonymous reviewers for their valuable comments and suggestions for the improvement of this manuscript. We thank the support of NOAA Climate Program Office (NA07OAR4310211 and NA10OAR4310170). This research was conducted under the CGIAR Research Program on Climate Change, Agriculture and Food Security (CCAFS); sub-contract with the International Potato Center (SB120184). L. Carvalho thanks FAPESP (2008/58101-9). NCEP Reanalysis data provided by the NOAA/OAR/ESRL PSD, Boulder, Colorado, USA, from their Web site at http://www.esrl.noaa.gov/psd. We thank NASA for making available the MERRA reanalysis, NOAA for making available GPCP and the SST data, and ANA for making available the precipitation station data. We also thank Dr. Brant Liebmann and Dr. David Allured for providing the precipitation station data and Dr. Hodges for his help with the spherical kernel technique.

References

Anderson TW, Finn JD (1996) The new statistical analysis of data. Springer, New York, p 712

Bombardi RJ, Carvalho LMV (2009) IPCC global coupled model simulations of the South America monsoon system. Climate Dyn 33:893–916. doi:10.1007/s00382-008-0488-1

Bombardi RJ, Carvalho LMV (2011) The South Atlantic dipole and variations in the characteristics of the South American Monsoon in the WCRP-CMIP3 multi-model simulations. Climate Dyn 36:2091–2102. doi:10.1007/s00382-010-0836-9

Cardoso ADO, Silva Dias PL (2004) Atlantic and Pacific variability and temperature during the winter season in Sao Paulo City. Revista Brasileira de Meteorologia 19:113–122

Carvalho LMV (2002) Intraseasonal large-scale circulations and mesoscale convective activity in tropical South America during the TRMM-LBA campaign. J Geophys Res 107:8042. doi:10.1029/2001JD000745

Carvalho LMV, Jones C, Liebmann B (2002) Extreme precipitation events in southeastern South America and large-scale convective patterns in the South Atlantic Convergence Zone. J Climate 15:2377–2394. doi:10.1175/1520-0442(2002)015<2377:EPEISS>2.0.CO;2

Carvalho LMV, Jones C, Liebmann B (2004) The South atlantic Convergence Zone: intensity, form, persistence, and relationships with intraseasonal to interannual activity and extreme rainfall. J Climate 17:88–108. doi:10.1175/1520-0442(2004)017<0088:TSACZI>2.0.CO;2

Carvalho LMV, Jones C, Ambrizzi T (2005) Opposite phases of the Antarctic oscillation and relationships with intraseasonal to interannual activity in the tropics during the Austral Summer. J Climate 18:702–718. doi:10.1175/JCLI-3284.1

Carvalho LMV, Silva AE, Jones C, Liebmann B, Silva Dias PL, Rocha HR (2010) Moisture transport and intraseasonal variability in the South America monsoon system. Climate Dyn 36:1865–1880. doi:10.1007/s00382-010-0806-2

Chaves RR, Nobre P (2004) Interactions between sea surface temperature over the South Atlantic Ocean and the South Atlantic Convergence Zone. Geophys Res Lett 31:L03204. doi:10.1029/2003GL018647

Da Silva AE, De Carvalho LMV (2007) Large-scale index for South America Monsoon (LISAM). Atmosph Sci Lett 8:51–57. doi:10.1002/asl.150

De Almeida RAF, Nobre P, Haarsma RJ, Campos EJD (2007) Negative ocean-atmosphere feedback in the South Atlantic Convergence Zone. Geophys Res Lett 34:L18809. doi:10.1029/2007GL030401

Doyle ME, Barros VR (2002) Midsummer low-level circulation and precipitation in subtropical South America and related sea surface temperature anomalies in the South Atlantic. J Clim 15:3394–3411

Gan MA, Rao VB (1991) Surface Cyclogenesis over South America. Mon Weather Rev 119:1293–1302. doi:10.1175/1520-0493(1991)119<1293:SCOSA>2.0.CO;2

Gan MA, Kousky VE, Ropelewski CF (2004) The South America Monsoon Circulation and Its Relationship to Rainfall over West-Central Brazil. J Climate 17:47–66. doi:10.1175/1520-0442(2004)017<0047:TSAMCA>2.0.CO;2

Grimm AM, Barros VR, Doyle ME (2000) Climate variability in Southern South America Associated with El Niño and La Niña Events. J Climate 13:35–58. doi:10.1175/1520-0442(2000)013<0035:CVISSA>2.0.CO;2

Grimm AM, Pal JS, Giorgi F (2007) Connection between Spring conditions and peak summer monsoon rainfall in South America: role of soil moisture, surface temperature, and topography in Eastern Brazil. J Climate 20:5929–5945. doi:10.1175/2007JCLI1684.1

Haarsma RJ (2003) Atmospheric response to South Atlantic SST dipole. Geophys Res Lett 30:1864. doi:10.1029/2003GL017829

Haarsma RJ, Campos EJD, Hazeleger W, Severijns C, Piola AR, Molteni F (2005) Dominant modes of variability in the South Atlantic: a study with a hierarchy of ocean–atmosphere models. J Climate 18:1719–1735. doi:10.1175/JCLI3370.1

Hartmann DL, Michelsen ML (1989) Intraseasonal peridiocities in Indian rainfall. J Atmos Sci 46:2838–2862. Available at: ftp://eos.atmos.washington.edu/pub/india-precip.pdf

Herdies DL (2002) Moisture budget of the bimodal pattern of the summer circulation over South America. J Geophys Res 107:8075. doi:10.1029/2001JD000997

Hodges KI (1996) Spherical nonparametric estimators applied to the UGAMP model integration for AMIP. Mon Weather Rev 124:2914–2932. doi:10.1175/1520-0493(1996)124<2914:SNEATT>2.0.CO;2

Hoskins BJ, Hodges KI (2005) A new perspective on southern hemisphere storm tracks. J Climate 18:4108–4129. doi:10.1175/JCLI3570.1

Jones C, Carvalho LMV (2002) Active and break phases in the South American Monsoon System. J Climate 15:905–914. doi:10.1175/1520-0442(2002)015<0905:AABPIT>2.0.CO;2

Kalnay E, Kanamitsu M, Kistler R et al. (1996) The NCEP/NCAR 40-year reanalysis project. Bull Am Meteorol Soc 77:437–471. doi:10.1175/1520-0477(1996)077<0437:TNYRP>2.0.CO;2

Kayano MT, Valéria Andreoli R, Ferreira de Souza RA (2011) Evolving anomalous SST patterns leading to ENSO extremes: relations between the tropical Pacific and Atlantic Oceans and the influence on the South American rainfall. Int J Climatol 31:1119–1134. doi:10.1002/joc.2135

Kayano MT, Andreoli R V., Ferreira de Souza R (2012) Relations between ENSO and the South Atlantic SST modes and their effects on the South American rainfall. Int J Climatol. n/a–n/a. doi:10.1002/joc.3569

Kodama Y (1992) Large-Scale common features of subtropical precipitation Zones (the baiu Frontal Zone, the SPCZ, and the SACZ) Part I: characteristics of Subtropical Frontal Zones. J Meteorol Soc Jpn 70:813–836

Kodama Y (1993) Large-Scale common features of subtropical precipitation zones (the baiu Frontal Zone, the SPCZ, and the SACZ) Part II: conditions of the circulations for generating the STCZs. J Meteorol Soc Jpn 71:581–610

Liebmann B, Kiladis GN, Marengo J, Ambrizzi T, Glick JD (1999) Submonthly convective variability over South America and the South Atlantic Convergence Zone. J Climate 12:1877–1891. doi:10.1175/1520-0442(1999)012<1877:SCVOSA>2.0.CO;2

Liebmann B, Jones C, De Carvalho LM V. (2001) Interannual variability of daily extreme precipitation events in the state of São Paulo, Brazil. J Clim 14:208–218. doi:10.1175/1520-0442(2001)014<0208:IVODEP>2.0.CO;2

Liebmann B, Kiladis GN, Vera CS, Saulo AC, Carvalho LM V. (2004) Subseasonal variations of rainfall in South America in the Vicinity of the low-level Jet East of the Andes and Comparison to Those in the South Atlantic Convergence Zone. J Climate 17:3829–3842. doi:10.1175/1520-0442(2004)017<3829:SVORIS>2.0.CO;2

Ma H-Y, Ji X, Neelin JD, Mechoso CR (2011) Mechanisms for precipitation variability of the Eastern Brazil/SACZ convective margin. J Climate 24:3445–3456. doi:10.1175/2011JCLI4070.1

Marengo JA, Soares WR, Saulo C, Nicolini M (2004) Climatology of the Low-Level Jet East of the Andes as derived from the NCEP–NCAR Reanalyses: Characteristics and Temporal Variability. J Climate 17:2261–2280. doi:10.1175/1520-0442(2004)017<2261:COTLJE>2.0.CO;2

Morioka Y, Tozuka T, Yamagata T (2011) On the growth and decay of the Subtropical Dipole Mode in the South Atlantic. J Climate 24:5538–5554. doi:10.1175/2011JCLI4010.1

Moura AD, Shukla J (1981) On the dynamics of droughts in Northeast Brazil: observations, theory and numerical experiments with a general circulation model. J Atmos Sci 38:2653–2675. doi:10.1175/1520-0469(1981)038<2653:OTDODI>2.0.CO;2

Murray RJ, Simmonds I (1991a) A numerical scheme for tracking cyclone centres from digital data Part I: development and operation of the scheme. Aust Meteorol Mag 39:155–166

Murray RJ, Simmonds I (1991b) A numerical scheme for tracking cyclone centres from digital data Part II: application to January and July general circulation model simulations. Aust Meteorol Mag 39:167–180

Muza MN, Carvalho LM V., Jones C, Liebmann B (2009) Intraseasonal and interannual variability of extreme dry and wet events over Southeastern South America and the Subtropical Atlantic during Austral Summer. J Climate 22:1682–1699. doi:10.1175/2008JCLI2257.1

Nnamchi HC, Li J, Anyadike RNC (2011) Does a dipole mode really exist in the South Atlantic Ocean? J Geophys Res 116: D15104. doi:10.1029/2010JD015579

Pezza AB, Ambrizzi T (2003) Variability of southern hemisphere cyclone and anticyclone behavior: further analysis. J Climate 16:1075–1083. doi:10.1175/1520-0442(2003)016<1075:VOSHCA>2.0.CO;2

Reboita MS (2008) Extratropical cyclones over the South Atlantic Ocean: climatic simulation and sensibility experiments. University of Sao Paulo, Sao Paulo, p 294

Reboita MS, Ambrizzi T, Rocha RP da (2009) Relationship between the southern annular mode and southern hemisphere atmospheric systems. Revista Brasileira de Meteorol 24:48–55.doi:10.1590/S0102-77862009000100005

Reboita MS, Da Rocha RP, Ambrizzi T, Sugahara S (2010) South Atlantic Ocean cyclogenesis climatology simulated by regional climate model (RegCM3). Climate Dyn 35:1331–1347. doi:10.1007/s00382-009-0668-7

Renwick JA (2005) Persistent positive anomalies in the southern hemisphere circulation. Mon Weather Rev 133:977–988. Available at: http://journals.ametsoc.org/doi/abs/10.1175/MWR2900.1. doi:10.1175/MWR2900.1

Reynolds RW, Smith TM, Liu C, Chelton DB, Casey KS, Schlax MG (2007) Daily high-resolution-blended analyses for sea surface

temperature. J Climate 20:5473–5496. doi:10.1175/2007JCLI1824.1

Rienecker MM, Suarez MJ, Gelaro R et al. (2011) MERRA: NASA's modern-era retrospective analysis for research and applications. J Climate 24:3624–3648. doi:10.1175/JCLI-D-11-00015.1

Robertson AW, Mechoso CR (2000) Interannual and interdecadal variability of the South Atlantic Convergence Zone. Mon Weather Rev 128:2947–2957. doi:10.1175/1520-0493(2000)128<2947:IAIVOT>2.0.CO;2

Robertson AW, Farrara JD, Mechoso CR (2003) Simulations of the atmospheric response to South Atlantic Sea surface temperature anomalies. J Climate 16:2540–2551. doi:10.1175/1520-0442(2003)016<2540:SOTART>2.0.CO;2

Rodrigues RR, Haarsma RJ, Campos EJD, Ambrizzi T (2011) The impacts of inter–El Niño variability on the tropical Atlantic and Northeast Brazil Climate. J Climate 24:3402–3422. doi:10.1175/2011JCLI3983.1

Saravanan R, Chang P (2000) Interaction between Tropical Atlantic Variability and El Niño–Southern Oscillation. J Climate 13:2177–2194. doi:10.1175/1520-0442(2000)013<2177:IBTAVA>2.0.CO;2

Simmonds I, Keay K (2000) Mean Southern hemisphere extratropical cyclone behavior in the 40-Year NCEP–NCAR Reanalysis. J Climate 13:873–885. doi:10.1175/1520-0442(2000)013<0873:MSHECB>2.0.CO;2

Sinclair MR (1996) A climatology of anticyclones and blocking for the Southern Hemisphere. Mon Weather Rev 124:245–264. doi:10.1175/1520-0493(1996)124<0245:ACOAAB>2.0.CO;2

Sterl A, Hazeleger W (2003) Coupled variability and air-sea interaction in the South Atlantic Ocean. Climate Dyn 21:559–571. doi:10.1007/s00382-003-0348-y

Taschetto AS, Wainer I (2008) The impact of the subtropical South Atlantic SST on South American precipitation. Ann Geophys 26:3457–3476. doi:10.5194/angeo-26-3457-2008

Torrence C, Compo GP (1998) A practical guide to wavelet analysis. bulletin of the American Meteorological Society 79:61–78. doi:10.1175/1520-0477(1998)079<0061:APGTWA>2.0.CO;2

Trenberth KE, Fasullo JT, Mackaro J (2011) Atmospheric moisture transports from ocean to land and global energy flows in reanalyses. J Climate 24:4907–4924. doi:10.1175/2011JCLI4171.1

Trzaska S, Robertson AW, Farrara JD, Mechoso CR (2007) South Atlantic variability arising from air–sea coupling: local mechanisms and tropical–subtropical interactions. J Climate 20:3345–3365. doi:10.1175/JCLI4114.1

Uvo CB, Repelli CA, Zebiak SE, Kushnir Y (1998) The relationships between Tropical Pacific and Atlantic SST and Northeast Brazil monthly precipitation. J Climate 11:551–562. doi:10.1175/1520-0442(1998)011<0551:TRBTPA>2.0.CO;2

Venegas SA, Mysak LA, Straub DN (1997) Atmosphere–ocean coupled variability in the South Atlantic. J Climate 10:2904–2920. doi:10.1175/1520-0442(1997)010<2904:AOCVIT>2.0.CO;2

Wilks DS (2006) Statistical methods in the atmospheric sciences. Academic Press, London, p 648

Xie P, Janowiak JE, Arkin PA et al. (2003) GPCP pentad precipitation analyses: an experimental dataset based on gauge observations and satellite estimates. J Climate 16:2197–2214. doi:10.1175/2769.1

Zhou J, Lau K-M (1998) Does a monsoon climate exist over South America? J Climate 11:1020–1040. doi:10.1175/1520-0442(1998)011<1020:DAMCEO>2.0.CO;2